AIAA JOURNAL
Vol. 40, No. 8, August 2002

Modulation of Near-Wall Turbulence Structure with Wall Blowing and Suction

Yongmann M. Chung*
University of Warwick, Coventry, England CV4 7AL, United Kingdom
Hyung Jin Sung†
Korea Advanced Institute of Science and Technology, Taejon 305-701, Republic of Korea
and
P.-Å. Krogstad‡
Norwegian University of Science and Technology, N-7491 Trondheim, Norway

The effects of wall blowing and suction on a fully developed, equilibrium turbulent channel flow are studied numerically. Direct numerical simulation data are analyzed to investigate the modulation of near-wall turbulence anisotropy after the sudden application of wall blowing and suction. The effects on the near-wall turbulence structure are examined in terms of the asymptotic near-wall behavior of various turbulence quantities and the turbulence anisotropy. It is found that blowing makes the near-wall flow more isotropic and enhances the transverse (v' and w') components of velocity fluctuations. A significant increase in the anisotropy of the near-wall region is found in the suction case. The anisotropy invariant map for the Reynolds stress anisotropy tensor indicates that the relaxation processes of the anisotropy of the near-wall turbulence are different for the blowing and suction cases, respectively. The response of the flow to the sudden application of wall blowing and suction occurs earlier for blowing than for suction, although there is a delayed response in both cases.

Nomenclature

b_{ij}	=	Reynolds stress anisotropy tensor, $\overline{u_i'u_j'}/2k - \delta_{ij}/3$
F	=	invariant function, $1 + 9II + 27III$
G	=	invariant function, $-(III/2)^2/(II/3)^3$
h	=	channel half-width
II	=	second invariants of b_{ij}, $-b_{ij}b_{ji}/2$
III	=	third invariants of b_{ij}, $b_{ij}b_{jk}b_{ki}/3$
k	=	turbulent kinetic energy, $\overline{u_k'u_k'}/2$
L_x, L_y, L_z	=	domain size in x, y, and z directions, respectively
Re_τ	=	Reynolds number, $u_\tau h/\nu$
U_m	=	bulk mean velocity
u, v, w	=	velocity components in x, y, and z directions, respectively
u_τ	=	friction velocity, $\sqrt{(\tau_w/\rho)}$, where $\tau_w = \mu\,(\mathrm{d}U/\mathrm{d}y)$
v_0	=	wall blowing and suction velocity
x, y, z	=	streamwise, normal, and spanwise coordinates
δ_{ij}	=	Kronecker delta
μ	=	dynamic viscosity
ν	=	kinematic viscosity
ρ	=	density
ω_i	=	$\sqrt{\omega_i'^2}$
ω_i'	=	vorticity fluctuations
ω_x'	=	streamwise vorticity fluctuations, $\mathrm{d}w'/\mathrm{d}y - \mathrm{d}v'/\mathrm{d}z$
ω_y'	=	normal vorticity fluctuations, $\mathrm{d}u'/\mathrm{d}z - \mathrm{d}w'/\mathrm{d}x$
ω_z'	=	spanwise vorticity fluctuations, $\mathrm{d}v'/\mathrm{d}x - \mathrm{d}u'/\mathrm{d}y$

Subscripts

in	=	inlet value
rms	=	root-mean-square value

Superscripts

$'$	=	fluctuation component
$+$	=	wall unit

I. Introduction

TURBULENT flow with wall blowing and suction has been investigated considerably over the past few decades.[1–17] Wall blowing and suction have been applied either uniformly in space[1–7] or locally through a thin slit over a limited spatial extent.[8–14] It is known that wall blowing and suction change several aspects of the flow. Wall blowing gives rise to an upward shift in the mean velocity logarithmic law, whereas a downward shift of the logarithmic velocity profile results from wall suction. The turbulent stresses are activated by wall blowing and decreased in the suction case.

It is evident that wall blowing and suction primarily affect the near-wall turbulence structure. In the blowing case, decreases in the turbulent length scales were observed experimentally by Krogstad and Kourakine[13,14] in a boundary layer with blowing through a slot. The Taylor microscale (see Ref. 14) and the mixing length scale[13] were reduced significantly as the blowing rate was increased. A decrease in the longitudinal integral length scale was found by Senda et al.[15] Sumitani and Kasagi[5] also observed streamwise vortical structures in smaller scales near the blowing wall in their direct numerical simulation (DNS). On the other hand, when wall suction was applied, an increased mean period of the bursting near the suction wall was found in the experiment of Elena.[16] Antonia et al.[2] observed a more orderly behavior of low-speed streaks and a greater longitudinal coherence of the low-speed streaks from visualizations of a turbulent boundary layer with uniform suction. The elongation of the low-speed streaks and the suppression of the spanwise meandering motion of the streaks were also observed in recent DNS study.[6,17] These findings imply that the anisotropy of the near-wall region can be significantly affected by the application of wall blowing and suction.

The interest in turbulence anisotropy is motivated not only by the better understanding of the turbulence structure but also by the

Received 27 May 2001; revision received 5 February 2002; accepted for publication 5 February 2002.

*Postdoctoral Researcher, Fluid Dynamics Research Centre, Department of Engineering.
†Professor, Department of Mechanical Engineering, 373-1 Kusong-dong, Yusong-ku; hjsung@kaist.ac.kr.
‡Professor, Department of Mechanics, Thermo and Fluid Dynamics.

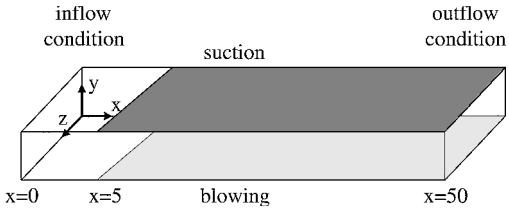

Fig. 1 Schematic diagram of flow configuration.

development of nonlinear turbulence models.[18] However, only a few studies on the anisotropy of turbulent flow with wall blowing and suction are available in the literature. The anisotropy of a turbulent boundary layer with uniform suction was investigated by Antonia et al.[19] by analyzing a DNS of Mariani et al.[4] They[19] found that the anisotropy increased significantly near the wall region when suction was applied at the wall. On the other hand, the effects of wall blowing on turbulence anisotropy is not conclusive,[13] although some experimental[15] and numerical[5,6] studies suggest that wall blowing makes the flow more isotropic.

The objective of the present study is, therefore, to investigate the effects of wall blowing and suction on turbulence anisotropy. The modulation of the turbulence structure is studied by analyzing DNS data. The databases used in the present study are obtained from DNS of a spatially developing turbulent channel flow.[6] A fully developed turbulent channel flow is subjected to sudden wall blowing and suction after an entrance section (Fig. 1). Uniform blowing is applied at the lower wall and uniform suction at the upper wall of the channel. The DNS used in this study is different from the previous DNS studies that dealt with a temporal simulation.[3–5] The temporal DNS presumes that the flow is homogeneous in the streamwise direction and applies periodic boundary conditions in that direction. Consequently, the turbulent flow with asymptotic wall blowing and suction was investigated in the previous DNS.

The modulation of the near-wall turbulence associated with uniform blowing and suction is examined in terms of the limiting behavior of turbulence intensities and the Reynolds stress anisotropy tensor. The anisotropy invariant map (AIM) for the Reynolds stress tensor is also analyzed. The instantaneous and time-mean velocity profiles and the turbulent kinetic energy budgets were published in an earlier paper by Chung and Sung.[6]

II. DNS Methods

In the DNS[6] that provides the data set employed in this analysis, the code developed by Yang and Ferziger[20] is used. Here, we only summarize the numerical method briefly.

The second-order accurate finite difference scheme is used for the convective and viscous terms. The solution procedure consists of a semi-implicit approach. A low-storage, third-order Runge–Kutta method is used for time integration for the nonlinear convective terms and a second-order Crank–Nicholson method for the viscous terms. The fractional-step method of Kim and Moin[21] is used to enforce the solenoidal condition. The resulting discrete Poisson equation for the pressure is solved using a discrete Fourier transformation in the spanwise direction and a pentadiagonal direct matrix solver in the wall-normal direction.

To impose a real turbulence at the inflow boundary, an auxiliary periodic DNS of a fully developed turbulent channel flow is performed concurrently with the main simulation.[22] The inflow simulation is matched to ensure that the meshing in all three directions and the time steps are identical to those of the main simulation. The flow is assumed to be periodic in the spanwise direction. A comprehensive description of the implementation of the inflow boundary condition may be found in Ref. 22.

In the present study, the Reynolds number is $Re_\tau = 150$, based on the channel half-width h and the wall friction velocity at inlet $u_{\tau_{\text{in}}}$. Wall blowing and suction are applied for $x > 5h$. The dimensionless wall transpiration velocity v_0^+ $(= v_0/u_{\tau_{\text{in}}})$ is set to be 0.05, and the resultant wall transpiration rate is $v_0/U_m = 0.0034$. The transpiration velocity is small and comparable to the one used experimentally by Antonia et al.[2] $(v_0^+ = 0.055)$ as well as computationally by Piomelli et al.[3] $(v_0/U_m = 0.004)$, Mariani et al.[4] $(v_0/U_m = 0.0036)$, and Sumitani and Kasagi[5] $(v_0^+ = 0.05)$.

The numerical parameters are chosen carefully through preliminary simulations.[10,11,17] The streamwise and spanwise dimensions of the computational domain are set such that $L_x = 51.2h$ and $L_z = 3h$, respectively. A $512 \times 129 \times 64$ grid system is used in the x, y, and z directions. The streamwise and spanwise grid resolutions are $\Delta x^+ = 15.0$ and $\Delta z^+ = 6.25$, respectively. The time step used is $\Delta t = 0.02h/U_m$, that is, $\Delta t^+ = 0.2$ in wall units. A detailed description of the numerical accuracy and grid independence as well as the numerical parameters used may be found in Ref. 6.

III. Results and Discussion

A. Vorticity Fluctuations

Figure 2 shows contours of the three components of the vorticity fluctuations, $\omega_i = \sqrt{\overline{\omega_i'^2}}$, where the prime indicates fluctuations about the mean value and overbar means averaging in time as well as in the spanwise direction. As seen, blowing and suction significantly modify the small-scale turbulent eddies. It is clear that the former enhances turbulence and that the latter suppresses it. Because the streamwise vortices are closely related to the near-wall turbulent activities, the response of the near-wall turbulence to blowing and suction can be explained in terms of the streamwise vortices.

Variations of the streamwise vorticity fluctuations at several streamwise locations are shown in Fig. 3. The location of the local maximum ω_x corresponds to the average location of the center of the streamwise vortices. The average size of the streamwise vortex can be estimated from the distance between the local maximum and minimum.[23] Because of the no-slip boundary condition, the streamwise vorticity with opposite sign is created at the wall, and the wall value of ω_x has an immediate response to wall perturbation.

As blowing and suction are applied at $x > 5$, the changes in ω_x distributions are shown first near the wall. At $x = 6$, ω_x decreases near the wall with blowing. Because $\omega_x' = \partial w'/\partial y$ at the wall (where w' is the spanwise velocity component), the decreases are attributed to the changes in w' (Ref. 9). As the flow goes downstream, the maximum value of ω_x increases slowly in the blowing case. Farther downstream, the streamwise vortices attain an asymptotic state at $x = 15$. The centers of the streamwise vortices are moved slightly toward the blowing wall, compared to the unperturbed flow.

In the suction case, the effects on the streamwise vorticity fluctuations are the opposite, with a slower response. Similar features are also observed in a DNS of Park and Choi,[12] where wall blowing and suction are applied through a spanwise slot. However, note that, in their DNS, the transpiration velocity was strong enough to push the streamwise vortices away from the wall in the blowing side, whereas, in the present DNS, the strength of the streamwise

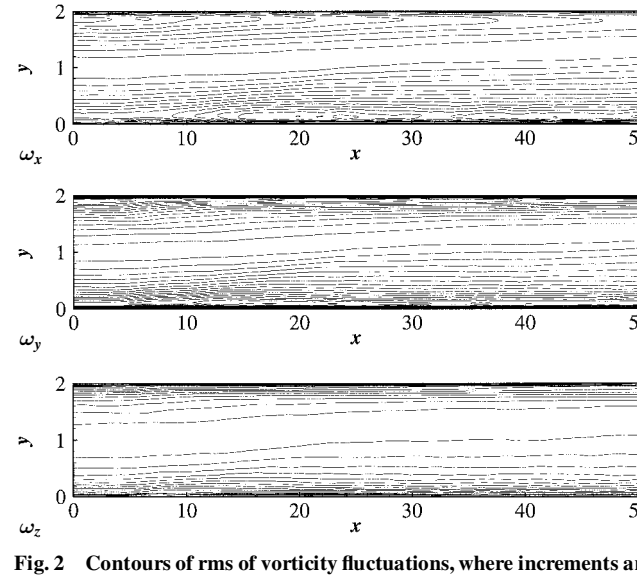

Fig. 2 Contours of rms of vorticity fluctuations, where increments are 0.1 for ω_x and ω_y and 0.2 for ω_z.

Table 1 Maximum values of vorticity fluctuations at exit

Vorticity fluctuation	Blowing[a]	Suction[a]
ω_x	1.38	0.48
ω_y	1.09	0.69
ω_z	1.03	0.79
ω_x at wall	1.42	0.45

[a]Values are normalized by the inlet value.

Table 2 Changes in the limiting values of turbulence intensities and Reynolds shear stress

Parameter	Blowing[a]	Suction[a]	Antonia et al.[20]
$u_{\rm rms}/y^+$	1.34	0.56	0.55
$v_{\rm rms}/y^{+2}$	2.60	0.18	0.14
$w_{\rm rms}/y^+$	1.94	0.31	0.26
$-\overline{u'v'}/y^{+3}$	3.10	0.12	0.11

[a]Values are normalized by the inlet value.

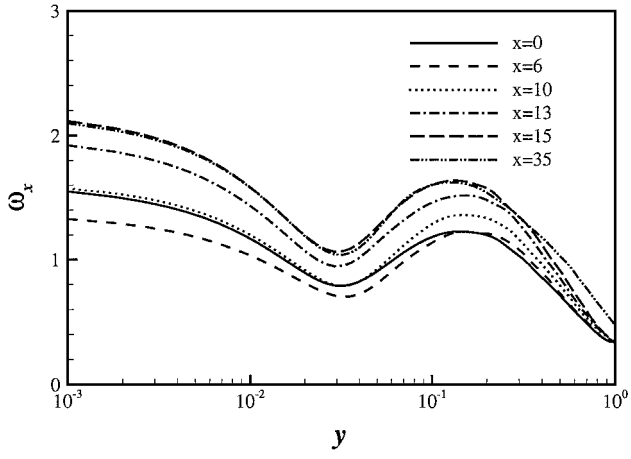

Blowing side

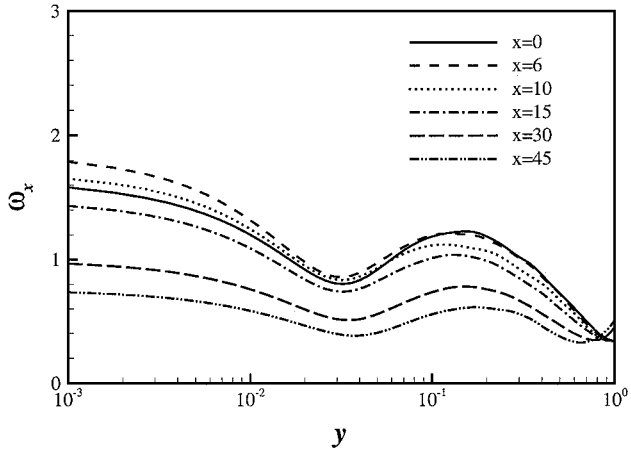

Suction side

Fig. 3 Variations of streamwise vorticity fluctuations at several streamwise locations.

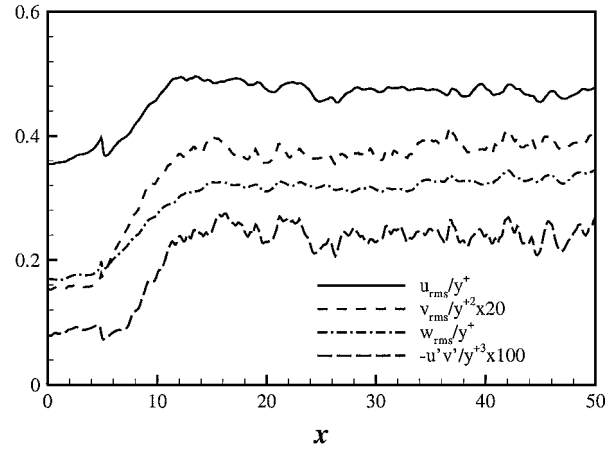

a) At the blowing wall

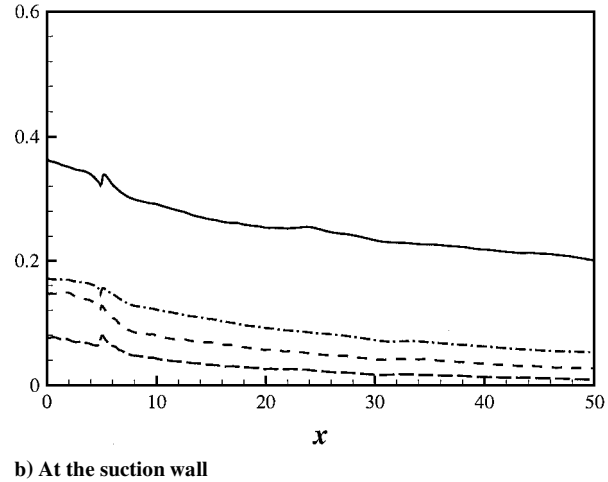

b) At the suction wall

Fig. 4 Distributions of the limiting behavior of the Reynolds stresses, $u_{\rm rms}/y^+$, $v_{\rm rms}/y^{+2} \times 20$, $w_{\rm rms}/y^+$, and $-\overline{u'v'}/y^{+3} \times 100$, where $y^+ = yu_\tau/\nu$ and u_τ is the local friction velocity along the wall.

vortices does not change quickly immediately after the application of blowing and suction.

The increases and decreases in the maximum values of ω_i near the exit, $x = 45$, are summarized in Table 1. The effects of wall transpiration are mainly on the streamwise vortices. When wall blowing is applied, ω_x increases by 38%, whereas the increases in ω_y and ω_z are only 9 and 3%, respectively. The decreases with suction are much larger than the increases with blowing. The strength of the streamwise vortices are decreased by more than half when suction is applied. When normalized by the wall variables ($\omega_x^+ = \omega_x \nu/u_\tau^2$), the increases with blowing and decreases with suction are amplified due to the changes in u_τ. Note u_τ decreases by 15% when blowing is applied and increases by 20% at the suction wall.[6] The changes in u_τ due to blowing and suction are in good agreement with those found in the temporal DNS.[5] Consequently, ω_x^+ increases by 90% with blowing and decreases by 67% with suction.

B. Limiting Behavior

Figure 4 shows the limiting behavior of turbulence intensities and Reynolds shear stress at the blowing and suction walls, respectively. Variables are normalized by the leading terms in the Taylor series expansion for each term: $u_{\rm rms}/y^+$, $v_{\rm rms}/y^{+2}$, $w_{\rm rms}/y^+$, and $-\overline{u'v'}/y^{+3}$. Note that, in Fig. 4, $v_{\rm rms}/y^{+2}$ and $-\overline{u'v'}/y^{+3}$ are multiplied by 20 and 100, respectively. The relaxation process associated with blowing is faster than that with suction. In the blowing case, all of the components approach an equilibrium state at around $x = 15$. Note that the limiting values at the blowing wall have a slightly faster response than the velocity fluctuations themselves. The maximum values of the velocity fluctuations have an equilibrium state at around $x = 20$ in Ref. 6. In contrast, suction has a slow relaxation, as shown in Fig. 4b. The blowing introduces a new inner layer that develops quickly because it is related to the inner variables, whereas suction continuously causes a diffusion toward the wall.

The increases with blowing and decreases with suction in the limiting values are summarized in Table 2. All of the limiting values are increased when blowing is applied. In the blowing case, $u_{\rm rms}/y^+$ is increased by about 34%, compared with about 160% for $v_{\rm rms}/y^{+2}$ and 94% for $w_{\rm rms}/y^+$. The amount by which $-\overline{u'v'}/y^{+3}$ is increased is even larger (210%) than that for $v_{\rm rms}/y^+$. Suction decreases the limiting values significantly. The effects of suction are more significant on the transverse v' and w' components of velocity fluctuations than on u'. The amount of decrease is in good agreement with the

DNS of a turbulent boundary layer with uniform suction.[19] The reduction in the near-wall value of $u_{\rm rms}/y^+$ also compares well with the data from experiments by Antonia et al.[2]

C. Turbulence Anisotropy

To assess the effects of wall blowing and suction on the turbulence structure, near-wall turbulence anisotropy is analyzed. A convenient way to characterize flow anisotropy is through the use of the Reynolds stress anisotropy tensor[24]:

$$b_{ij} = \overline{u_i' u_j'}/2k - \delta_{ij}/3 \tag{1}$$

where summation over repeated indices is implied. The second and third invariants of the Reynolds stress anisotropy tensor b_{ij} are given by

$$II = -\tfrac{1}{2} b_{ij} b_{ji} \tag{2}$$

$$III = \tfrac{1}{3} b_{ij} b_{jk} b_{ki} \tag{3}$$

Contour lines of the Reynolds stress anisotropy tensor b_{12} and the second invariant $-II$ are shown in Fig. 5. It is known that, when a fully developed turbulent wall-bounded flow is subjected to a sudden wall blowing and suction, there is an initial relaxation from the upstream impermeable wall boundary condition toward an equilibrium state after the step change in wall boundary condition.[6,17,25,26] Although wall blowing and suction are applied from $x = 5$, it is found that there is a delay in the response of the near-wall anisotropy to the sudden application of wall blowing and suction. The effects of blowing and suction on the near-wall turbulence are seen in b_{12} from $x = 15$. The activation of the turbulent motions by blowing and the suppression by suction are reflected in the changes in b_{12}. In the near-wall region, a faster response of $-II$ to wall blowing is shown compared to wall suction, and the changes in the second invariant are also discernible at $x = 15$ (Fig. 6).

Figure 6 shows the variations of $-II$ at several streamwise locations. It is clear that blowing decreases $-II$ and makes the flow more isotropic in the logarithmic layer. The magnitude of $-II$ decreases over most of the channel, except for the core region, $y > 0.6$, where it decreases slightly. The decreased anisotropy is attributed to the activated v' and w' components. When suction is applied, the anisotropy is improved. A substantial decrease in the v' and w' components, which is responsible for the enhanced anisotropy with suction, is observed by Chung and Sung.[6] Isotropy is slightly improved in the core region, and the same trend is observed in a boundary layer DNS by Antonia et al.[19] The faster response of $-II$ to blowing is clearly seen, which is consistent with the limiting behavior in Fig. 4. The overall behavior of III (not shown here) is found to be very similar to the behavior of $-II$.

Each component of the Reynolds stress anisotropy tensor b_{ij} at several streamwise locations is shown in Figs. 7 and 8 for the blowing and suction cases, respectively. The most distinct effects of the blowing and suction in the near-wall region are observed in b_{33}: In the blowing case, the near-wall value of b_{33} is closer to the isotropic

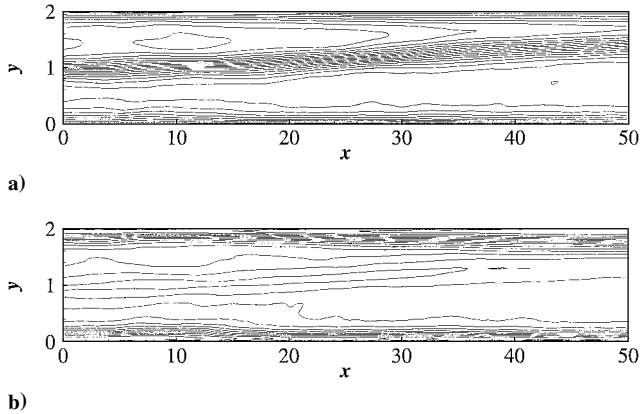

Fig. 5 Variations where increments are 0.02 of a) the Reynolds stress anisotropy tensor b_{12} and b) the second invariant $-II$.

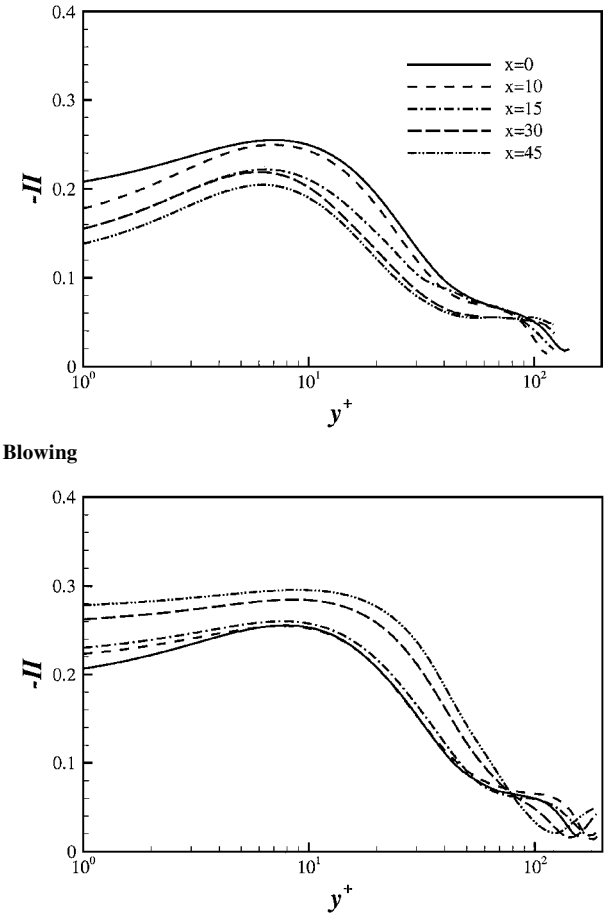

Fig. 6 Anisotropy invariant $-II$.

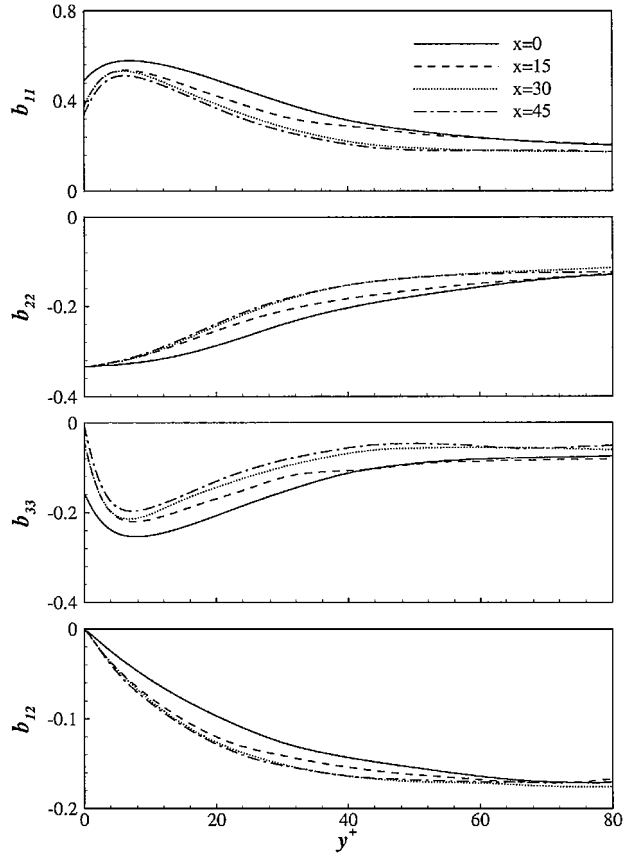

Fig. 7 Reynolds stress anisotropy tensor b_{ij} at several streamwise locations in the blowing case.

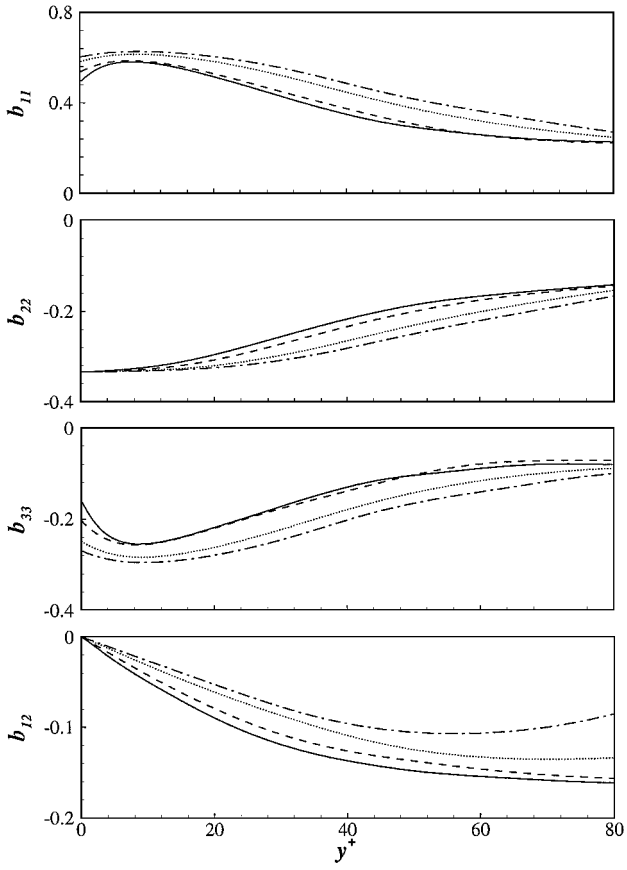

Fig. 8 Reynolds stress anisotropy tensor b_{ij} at several streamwise locations in the suction case.

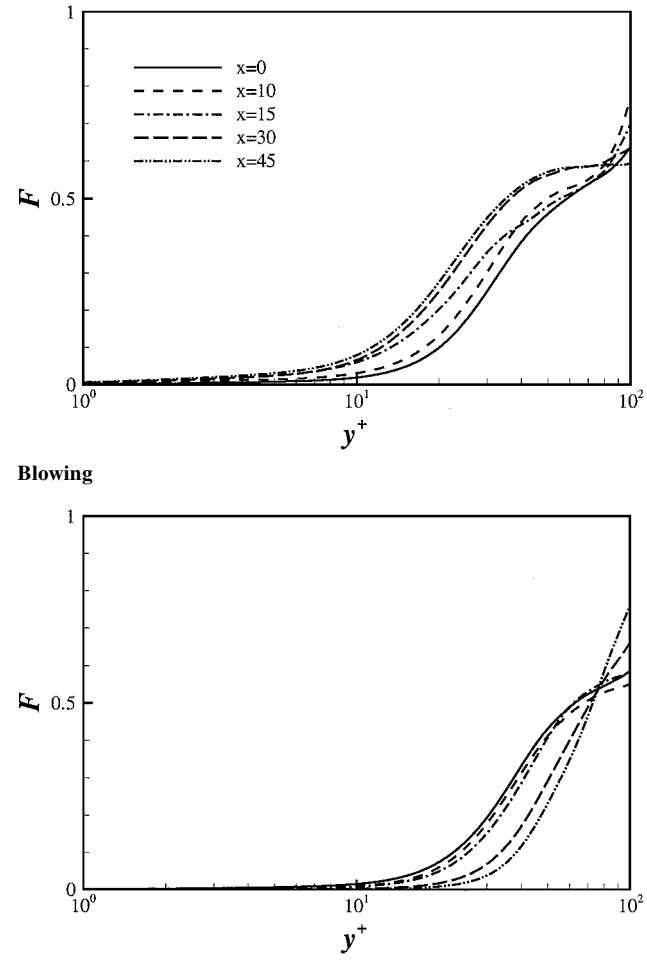

Fig. 9 Anisotropy invariant function $F = 1 + 9II + 27III$.

state $b_{33} = 0$, whereas b_{33} changes by 50% in the suction case. The faster response of b_{ij} to blowing is clearly seen from the data at $x = 15$. The decrease of b_{11} and the increase of b_{22} and b_{33} in the blowing case are attributed to the enhanced transverse v' and w' components of velocity fluctuations.[6] The absolute value of b_{12} increases when blowing is applied, and this indicates the activated turbulent motions with blowing. In the suction case, the early response of b_{ij} is very slow, and b_{ij} does not change much at $x = 15$. The decrease in absolute value of b_{12} shows the suppression of the turbulence activities by suction. The enhanced anisotropy in the wall region with suction is also found in the experiment of Antonia et al.[2] and DNS boundary-layer flow data.[19]

Two invariant functions are examined in this study:

$$F = 1 + 9II + 27III \tag{4}$$

$$G = -(III/2)^2/(II/3)^3 \tag{5}$$

The first function represents the two-component turbulent state and F should go to zero near the wall. Without blowing and suction, near the wall, the velocity component normal to the wall, v', is suppressed by the "splatting" phenomenon,[23,24] and the turbulence approaches the two-component state. The second function represents the axisymmetric turbulent state and the ratio should be 1. As shown in Fig. 9, in the blowing case, the two-component turbulent state region is decreased significantly. On the other hand, suction increases the two-component turbulent state region substantially. These features are attributed mainly to the changes in b_{22} with blowing and suction near the wall. Note that when suction is applied b_{22}, at $x = 45$, is almost zero for $y^+ < 20$. The ratio G deviates from the unity when blowing is applied (Fig. 10). In the suction case, the region for the axisymmetric turbulent state is elongated substantially. The ratio is about 0.99 in the range $5 < y^+ < 20$ at $x = 45$. Similar features are observed by Antonia et al.[19] The ratio is about 0.98 in their study for $3 < y^+ < 20$.

D. AIM

Lumley and Newman[27] have shown that the cross plots of the invariants $-II$ and III for axisymmetric turbulence and for two-component turbulence define the AIM that bounds all physically realizable turbulence. In the AIM, turbulence must exist within the area surrounded by three lines. The upper straight line $II + 3III + \frac{1}{9} = 0$ represents a state of two-component turbulence. The right and left boundaries of the AIM ($-II^3/3^3 = III^2/2^2$) identify the prolate and the oblate axisymmetric turbulent states, respectively. The right vertex of the AIM ($-II = \frac{1}{3}$, $III = \frac{2}{27}$) indicates one-component turbulence. The bottom cusp ($II = 0$, $III = 0$) characterizes the isotropic state of turbulence.

Figure 11 shows the AIM for the Reynolds stress tensor at inflow. The invariant data from a homogeneous channel flow DNS of Kuroda et al.[28] are also included for comparison. The present data show all of the characteristics of the near-wall turbulence anisotropy and are in good agreement with the temporal DNS data.[28] Without blowing and suction, turbulence in a plane channel flow varies from a two-component turbulent state near the wall to a nearly isotropic state in the core region. At around the boundary of the viscous sublayer, the anisotropy tensor is closest to the one-component state.

The downstream relaxation of the turbulence anisotropy is examined in some detail. The AIMs at two downstream locations, $x = 15$ and 30, are shown in Fig. 12. It is clearly seen in Fig. 12a that the flow becomes more isotropic when blowing is applied (compare Fig. 11). The early response of the near-wall anisotropy to blowing is substantial. At $x = 15$, the anisotropy data are shifted to the left in the AIM from the inlet values. This feature is consistent with the activated transverse components of velocity fluctuations observed by Chung and Sung.[6] To assess the changes in the AIM, the maximum values of $-II$ and III are monitored. The maximum values of $-II$ and III at several streamwise locations are summarized in

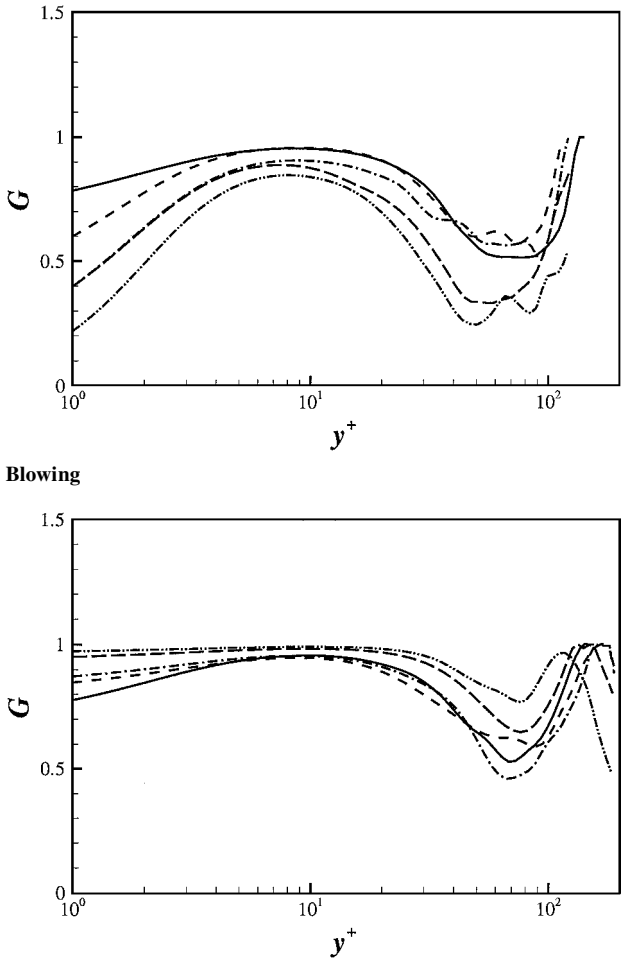

Fig. 10 Anisotropy invariant function $G = -(III/2)^2/(II/3)^3$.

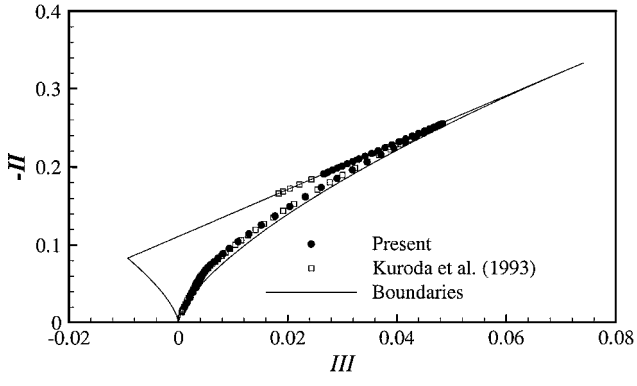

Fig. 11 Anisotropy invariant map for the Reynolds stress tensor at inflow.

Table 3. At $x = 15$, the maximum values of $-II$ and III in the blowing case are decreased by 13 and 21%, respectively. These values correspond to two-thirds of the total decrease obtained at the exit of the computational domain. Farther downstream, at $x = 30$, the effect of blowing on the anisotropy tensor is mild compared with the strong early response at $x = 15$.

The relaxation processes of the near-wall anisotropy in the blowing and suction cases are different from each other. In the suction case, the early response of the near-wall anisotropy is rather slow. At $x = 15$, the AIM in the suction case shows little change from the inlet values shown in Fig. 11. Farther downstream, at $x = 30$, however,

Table 3 Maximum values of $-II$ and III at several streamwise locations in the blowing case

Invariant[a]	$x = 0$	$x = 15$	$x = 30$	$x = 45$
$-II_B$	0.255	0.221	0.217	0.204
III_B	0.0484	0.0380	0.0367	0.0324
$-II_S$	0.255	0.260	0.284	0.295
III_S	0.0484	0.0498	0.0579	0.0614

[a]Subscript B indicates values in the blowing side and S in the suction side.

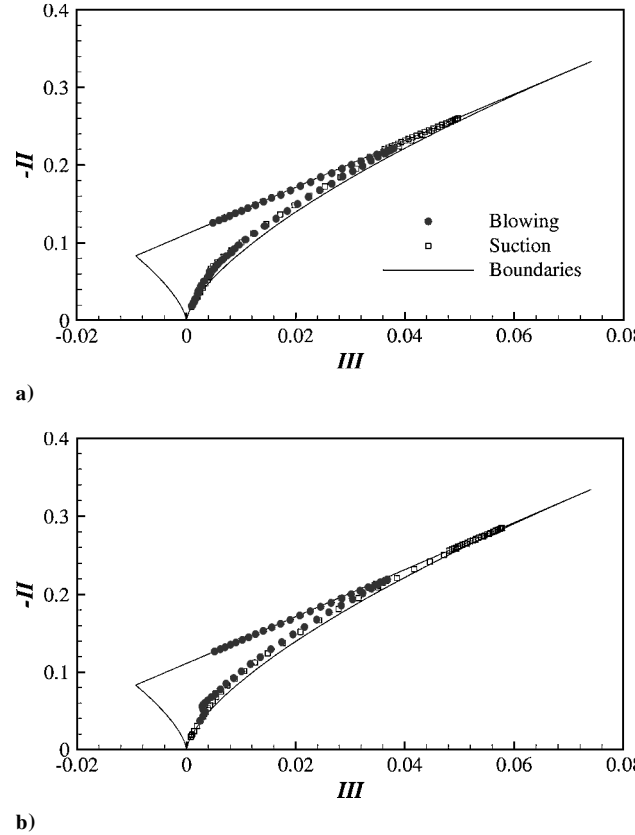

Fig. 12 Anisotropy invariant map for blowing at a) $x = 15$ and b) $x = 30$.

the turbulence becomes more anisotropic and the Reynolds stress tensor begins to approach the right-hand-side vertex corresponding to the one-component turbulence. The maximum values of $-II$ and III at $x = 30$ are increased by 11 and 20%. The slow response of the anisotropy is also seen in the Reynolds stress anisotropy tensor b_{ij} shown in Fig. 8.

The different responses of turbulence anisotropy to wall blowing and suction are clear in Fig. 13, which shows the AIM near the exit of the computational domain, at $x = 45$. The invariant data calculated from a temporal DNS[5] are also included for comparison. The trends observed in Fig. 12 are manifested in Fig. 13. It appears that the anisotropy tensor of near-wall turbulence approaches its asymptotic value near the exit. The near-wall value at the suction wall approaches a right-hand-side vertex corresponding to the one-component turbulence. The maximum values of $-II$ and III in the suction case are very close to the coordinates of the top vertex (Table 3). The maximum values of $-II$ and $-III$ decrease by 20 and 33% in the blowing case and increase by 15 and 27% in the suction case, respectively. This is fairly close to the asymptotic values obtained from the periodic DNS of Sumitani and Kasagi.[5] In their DNS, the decrease in the blowing case was 22 and 36%, and the increase was 14 and 24% in the suction case, compared to the no blowing/suction case.[28]

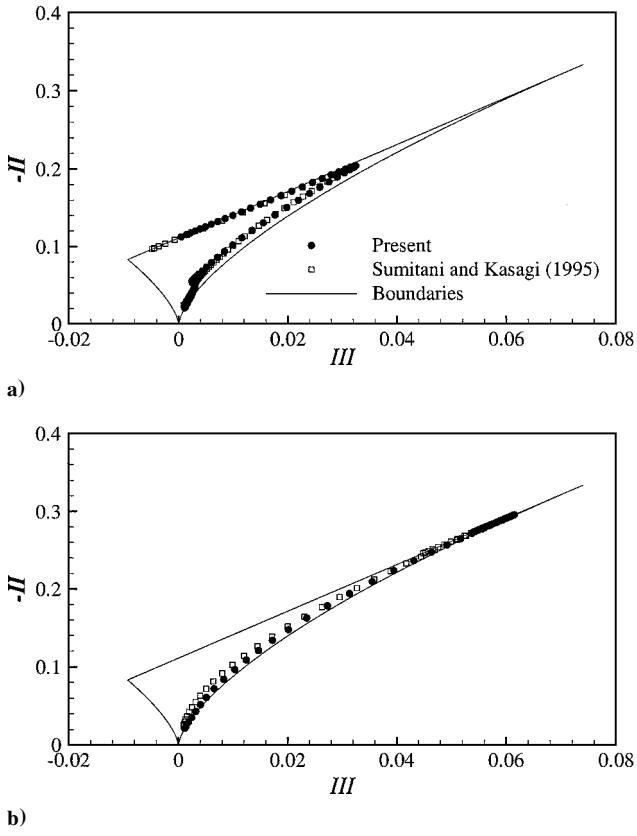

Fig. 13 Anisotropy invariant map for suction at a) $x = 15$ and b) $x = 30$.

IV. Conclusions

DNS data of a spatially developing turbulent channel flow are analyzed to investigate the modulation of the near-wall turbulence with uniform wall blowing and suction. It is found that blowing activates the transverse v' and w' components of velocity fluctuations and decreases the anisotropy of the near-wall turbulence significantly. When suction is applied, turbulence becomes much more anisotropic, and the near-wall values approach the one-component turbulence limit. Previous findings that suggest the effects of wall blowing and suction on the near-wall turbulence structure are corroborated in the present study. After the sudden application of wall blowing and suction, there is a delay in the response of the near-wall anisotropy to the sudden change. A study of the AIM indicates that the response of near-wall anisotropy to blowing is faster than the response to suction. The early response of the near-wall anisotropy to blowing is clearly observed in the b_{33} component of the Reynolds stress anisotropy tensor. The region for the two-component turbulent state near the wall is enlarged when suction is applied. Axisymmetric turbulent state region is also increased with suction.

Acknowledgments

This research was supported partially by a grant from the National Research Laboratory of the Ministry of Science and Technology, Republic of Korea. The authors are grateful to Nigel Prentice for reading the manuscript.

References

[1]Simpson, R. L., "Characteristics of Turbulent Boundary Layer at Low Reynolds Numbers with and without Mass Transpiration," *Journal of Fluid Mechanics*, Vol. 42, 1970, pp. 769–802.

[2]Antonia, R. A., Fulachier, L., Krishnamoorthy, L. V., Benabid, T., and Anselmet, F., "Influence of Wall Suction on the Organized Motion in a Turbulent Boundary Layer," *Journal of Fluid Mechanics*, Vol. 190, 1988, pp. 217–240.

[3]Piomelli, U., Ferziger, J. H., and Moin, P., "New Approximate Boundary Conditions for Large Eddy Simulations of Wall-Bounded Flows," *Physics of Fluids A*, Vol. 1, No. 6, 1989, pp. 1061–1068.

[4]Mariani, P., Spalart, P. R., and Kollmann, W., "Direct Simulation of a Turbulent Boundary Layer with Suction," *Near-Wall Turbulent Flows*, edited by R. M. C. So, C. G. Speziale, and B. E. Launder, Elsevier, Amsterdam, 1993, pp. 347–356.

[5]Sumitani, Y., and Kasagi, N., "Direct Numerical Simulation of Turbulent Transport with UniformWall Injection and Suction," *AIAA Journal*, Vol. 33, No. 7, 1995, pp. 1220–1228.

[6]Chung, Y. M., and Sung, H. J., "Initial Relaxation of Spatially Evolving Turbulent Channel Flow Subjected to Wall Blowing and Suction," *AIAA Journal*, Vol. 39, No. 11, 2001, pp. 2091–2099.

[7]Chung, Y. M., and Sung, H. J., "Modulation of Near-Wall Anisotropy with Uniform Wall Blowing and Suction," *Turbulence and Shear Flow Phenomena—2*, edited by E. Lindborg, A. Johansson, J. Eaton, J. Humphrey, N. Kasagi, M. Leschziner, and M. Sommerfeld, Vol. 2, Universitetsservice US AB, Stockholm, 2001, pp. 317–322.

[8]Sano, M., and Hirayama, N., "Turbulent Boundary Layers with Injection and Suction Through a Slit. First Repost: Mean and Turbulence Characteristics," *Bulletin of Japanese Society of Mechanical Engineers*, Vol. 28, No. 239, 1985, pp. 807–814.

[9]Antonia, R. A., Zhu, Y., and Sokolov, M., "Effect of Concentrated Wall Suction on a Turbulent Boundary Layer," *Physics of Fluids*, Vol. 7, No. 10, 1995, pp. 2465–2474.

[10]Chung, Y. M., and Sung, H. J., "Effects of Local Blowing on Spatially-Evolving Turbulent Channel Flow," *Proceedings of the Fourth KSME-JSME Fluids Engineering Conference*, Pusan, Republic of Korea, 1998, pp. 673–676.

[11]Chung, Y. M., and Sung, H. J., "Asymmetric Response of Turbulent Channel Flow to Wall Suction and Blowing," *Turbulence and Shear Flow Phenomena—1*, edited by S. Banerjee and J. K. Eaton, Begell House, New York, 1999, pp. 423–428.

[12]Park, J., and Choi, H., "Effects of Uniform Blowing or Suction From a Spanwise Slot on a Turbulent Boundary Layer Flow," *Physics of Fluids*, Vol. 11, No. 10, 1999, pp. 3095–3105.

[13]Krogstad, P.-Å., and Kourakine, A., "Some Effects of Localized Injection on the Turbulence Structure in a Boundary Layer," *Physics of Fluids*, Vol. 12, No. 11, 2000, pp. 2990–2999.

[14]Krogstad, P.-Å., and Kourakine, A., "The Response of a Turbulent Boundary Layer to Injection Through a Porous Strip," *Turbulence and Shear Flow Phenomena—1*, edited by S. Banerjee and J. K. Eaton, Begell House, New York, 1999, pp. 429–434.

[15]Senda, M., Kawaguchi, Y., Suzuki, K., and Sato, T., "Study on Turbulent Boundary Layer with Injection," *Bulletin of Japanese Soceity of Mechanical Engineers*, Vol. 24, No. 196, 1981, pp. 1748–1755.

[16]Elena, M., "Suction Effects on Turbulence Statistics in a Heated Pipe Flow," *Physics of Fluids*, Vol. 27, No. 4, 1984, pp. 861–866.

[17]Chung, Y. M., Sung, H. J., and Luo, K. H., "Response of Turbulent Channel Flow to Sudden Wall Suction and Blowing," *Advances in Turbulence VIII*, edited by C. Dopazo, International Center for Numerical Methods in Engineering, Barcelona, Spain, 2000, pp. 109–112.

[18]Gatski, T. B., Hussaini, M. Y., and Lumley, J. L., *Simulation and Modeling of Turbulent Flows*, Oxford Univ. Press, Oxford, 1996, pp. 185–242.

[19]Antonia, R. A., Spalart, P. R., and Mariani, P., "Effect of Suction on the Near-Wall Anisotropy of a Turbulent Boundary Layer," *Physics of Fluids*, Vol. 6, No. 1, 1994, pp. 430–432.

[20]Yang, K.-S., and Ferziger, J. H., "Large-Eddy Simulation of Turbulent Obstacle Flow Using a Dynamic Subgrid-Scale Model," *AIAA Journal*, Vol. 31, No. 8, 1993, pp. 1406–1413.

[21]Kim, J., and Moin, P., "Application of a Fractional-Step Method to Incompressible Navier–Stokes Equations," *Journal of Computational Physics*, Vol. 59, No. 2, 1985, pp. 308–323.

[22]Chung, Y. M., and Sung, H. J., "Comparative Study of Inflow Conditions for Spatially Evolving Simulation," *AIAA Journal*, Vol. 35, No. 2, 1997, pp. 269–274.

[23]Kim, J., Moin, P., and Moser, R., "Turbulence Statistics in Fully Developed Channel Flow at Low Reynolds Number," *Journal of Fluid Mechanics*, Vol. 177, 1987, pp. 133–166.

[24]Mansour, N. N., Kim, J., and Moin, P., "Reynolds-Stress and Dissipation-Rate Budgets in a Turbulent Channel Flow," *Journal of Fluid Mechanics*, Vol. 194, 1988, pp. 15–44.

[25]Smits, A. J., and Wood, D. H., "The Response of Turbulent Boundary Layers to Sudden Perturbations," *Annual Review of Fluid Mechanics*, Vol. 17, 1985, pp. 321–358.

[26]Bushnell, D. M., and McGinley, C. B., "Turbulence Control in Wall Flows," *Annual Review of Fluid Mechanics*, Vol. 21, 1989, pp. 1–20.

[27]Lumley, J. L., and Newman, G. R., "The Return to Isotropy of Homogeneous Turbulence," *Journal of Fluid Mechanics*, Vol. 82, 1979, pp. 161–178.

[28]Kuroda, N. N., Kasagi, N., and Hirata, M., "Direct Numerical Simulation of Turbulent Plane Couette–Poiseuille Flows: Effect of Mean Shear Rate on the Near-Wall Turbulence Structures," *Turbulence Shear Flows 9*, edited by F. Durst, N. Kasagi, B. E. Launder, F. W. Schmidt, K. Suzuki, and J. H. Whitelaw, Springer-Verlag, Berlin, 1995, pp. 241–257.

P. Givi
Associate Editor